Original Investigation

Photon-Counting Detector CT for Kidney Stone Detection in Excretory Phase CT—Comparison Between Virtual Non-contrast and Virtual Non-iodine Reconstructions in a 3D Printed Kidney Phantom

Philipe S. Breiding, MD, EBIR, Ana Maria Turrion Gomollon, MD, Katharina Martini, MD, Dominik Nakhostin, MD, Hatem Alkadhi, MD, MPH, EBCR, FESER, André Euler, MD, EBCR, MHBA

Rationale and Objectives: To evaluate and compare the effectiveness of contrast media subtraction and kidney stone detection between a virtual non-iodine reconstruction algorithm (VNI; PureCalcium) and a virtual non-contrast (VNC) algorithm in excretory phase photon-counting detector computed tomography (PCD-CT), using a 3D printed kidney phantom under various tube voltages and radiation doses.

Materials and Methods: A 3D-printed kidney phantom, holding Calcium Oxalate (CaOx) and uric acid stones within contrast-enhanced calyces, was created. The calyx density mirrored the average density observed in 200 excretory phase patients (916 HU at 110 kV). Imaging was conducted on a clinical dual-source PCD-CT at 120 kV and 140 kV, with radiation doses set at 5, 10, and 15 mGy. VNI and VNC algorithms were applied. Two blinded readers evaluated the image quality, along with the degree of contrast media and kidney stone subtraction, using visual scales. Krippendorff's alpha was calculated to determine inter-reader agreement, and the Chi-squared test was employed for comparing ordinal data.

Results: Reader 2 rated overall image quality higher for VNI than VNC (4.90 vs. 4.00; $P < .05$), while Reader 1 found no significant difference (4.96 vs. 5.00; $P > .05$). Substantial agreement was observed between readers for contrast media subtraction in both VNC and VNI (Krippendorff's alpha range: 0.628–0.748). Incomplete contrast media subtraction occurred more frequently with VNI for both readers (Reader 1: 29% vs. 15%; $P < .05$; Reader 2: 24% vs. 20%; $P > .05$). Uric acid and smaller stones (< 5 mm) were more likely to be subtracted than CaOx and larger stones in both VNC and VNI. Overall, a higher rate of stone subtraction was noted with VNI compared to VNC (Reader 1: 22% vs. 16%; Reader 2: 25% vs. 10%; $P < .05$). Neither radiation dose nor tube voltage significantly influenced stone subtraction ($P > .05$).

Conclusion: VNC demonstrated greater accuracy than VNI for contrast media subtraction and kidney stone visibility. Radiation dose and tube voltage had no significant impact. Nonetheless, both algorithms still exhibited frequent incomplete contrast media subtraction and partial kidney stone subtraction.

Key Words: Kidney; Kidney stones; Phantom; Photon-counting CT; Virtual non-iodine; Virtual non-contrast; PureCalcium; Radiation dose; Image reconstruction.

Acad Radiol xxxx; xx:xxx–xxx

From the Diagnostic and Interventional Radiology, University Hospital Zurich, University of Zurich, Zurich, Switzerland; University Institute of Diagnostic and Interventional Neuroradiology, Inselspital, University of Bern, Bern, Switzerland; Department of Radiology, Kantonsspital Baden, Baden, Switzerland. Received February 24, 2024; revised March 24, 2024; accepted April 4, 2024. **Address correspondence to**: A.E. e-mail: and.euler@gmail.com

https://doi.org/10.1016/j.acra.2024.04.002

INTRODUCTION

Hematuria is a common clinical symptom with a prevalence of microhematuria of up to 31%. (1,2) In patients with risk factors presenting with microhematuria and in patients presenting with gross hematuria, a multi-phase computed tomography (CT) scan, including unenhanced, venous, and excretory phases, is usually considered appropriate in order to exclude urolithiasis and malignancies in the kidneys and upper urinary tract (2). Given the radiation risk associated with multi-phase CT imaging, there is an increasing focus on developing strategies to reduce scan acquisitions, thereby aiming to lessen radiation exposure to patients. A promising strategy to reduce the number of acquisitions involves employing virtual non-contrast (VNC) imaging derived from dual-energy CT (DECT), as an alternative to actual unenhanced images. Former studies have shown that by omitting the true non-contrast (TNC) phase, the radiation dose can be reduced by an average of 28% ± 6% using conventional energy-integrating detector DECT (3). Nevertheless, numerous studies have indicated the inadvertent subtraction of smaller stones in virtual unenhanced images (3–7).

Photon-counting detector CT (PCD-CT) is an emergent technology with potential benefits over traditional energy-integrating detector CT, including reduced image noise, enhanced contrast and spatial resolution, and greater radiation dose efficiency (8). Unlike conventional energy-integrating CT, PCD-CT enables the application of an energy-dependent weighting factor, enhancing signal-to-noise ratio and broadening energy discrimination for detailed information on the elemental composition of the imaged substances (9–11). Currently, two algorithms are available for iodine subtraction in PCD-CT: VNC and virtual non-iodine (VNI; PureCalcium (PC), Siemens Healthineers). Both reconstruction techniques offer the ability to generate images that mimic those obtained from a true non-contrast CT scan. VNI uses iodine and calcium while VNC uses iodine and water as base materials for the material decomposition. VNI permits the removal of iodine contrast without compromising calcium contrast, a limitation in traditional VNC imaging. Applied during the excretory phase, these techniques could potentially supplant the true unenhanced CT in multi-phase imaging of the urinary tract, thus reducing overall patient radiation exposure. Currently, the efficacy of VNI and VNC in eliminating iodinated contrast media and detecting kidney stones in excretory phase CT of the upper urinary tract remains unexplored.

Hence, this study aimed to evaluate the accuracy of contrast media subtraction and kidney stone detection between VNI and VNC in excretory phase PCD-CT, utilizing a 3D-printed kidney phantom across varying tube voltages and radiation doses.

MATERIALS AND METHODS

Kidney Stones

Kidney stones of varying sizes were collected by means of endoscopic retrieval, self-straining through a collecting sieve, or by urological surgery. Stones were characterized using X-ray diffraction and were categorized and sorted according to their main composition. We included a total of 5 uric acid and 5 calcium oxalate (CaOx) stones with similar sizes of 2 mm, 3 mm, 4 mm, 5 mm and 10 mm. The stones were measured with a physical ruler and the correct size was confirmed using the measuring tool in the CT images. All stones varied considerably in their shape, with some being almost perfectly round while others were spiculated or oval.

Determination of Renal Calyx Density in the Excretory Phase

The average intraluminal renal calyx density in the contrast-enhanced excretory phase was retrospectively measured by a single-blinded radiologist (D.N., board-certified radiologist with 6 years of experience with multi-energy CT) in 200 consecutive patients imaged between 2015 and 2020 at a tube voltage of 110 kV on a dual-source dual-energy CT (SOMATOM Force, Siemens Healthineers, Forchheim, Germany). The reader was asked to place a single ROI (region of interest) in the visually dominant calyx. All patients received the institutional standard renal scan protocol, with the excretory phase being acquired 10 minutes after contrast media injection. Patients were not routinely administered diuretics prior to CT imaging. The average renal calyx density measured 916 HU ± 342 HU in the excretory phase.

Phantom Design

A custom kidney phantom was fabricated using a 3D printer (Fig 1). The phantom was composed of hardened polylactic acid and included a hollow chamber with a volume of 600 mL as well as five fillable cylinders (length, 80 mm in the z-direction; diameter, 25 mm) to hold the individual kidney stones. The hollow chamber was filled with distilled water and all cylinders were filled with iodinated contrast media solutions which had a similar density to the mean density measured in patients (916 HU). The iodinated solutions were prepared by mixing distilled water with iopromide (Ultravist 300, 300 mgI/mL, Bayer, Berlin, Germany). A single kidney stone was placed into each individual cylinder and the phantom was placed inside one ring of fat-equivalent material (8 cm thickness) to simulate a medium-sized patient. No calyx was left empty.

Image Acquisition

All scans were performed on a clinical first-generation dual-source PCD-CT (NAEOTOM Alpha, Siemens Healthcare GmbH, Forchheim, Germany, Syngo CT VA50). All scans were obtained in the multi-energy mode (QuantumPlus) at a tube voltage of 120 kV and 140 kV, a collimation of 144 × 0.4 mm, a gantry rotation time of 0.25 s and a spiral pitch factor of 1.2. The image quality level was adjusted to achieve a radiation dose with a volumetric dose index

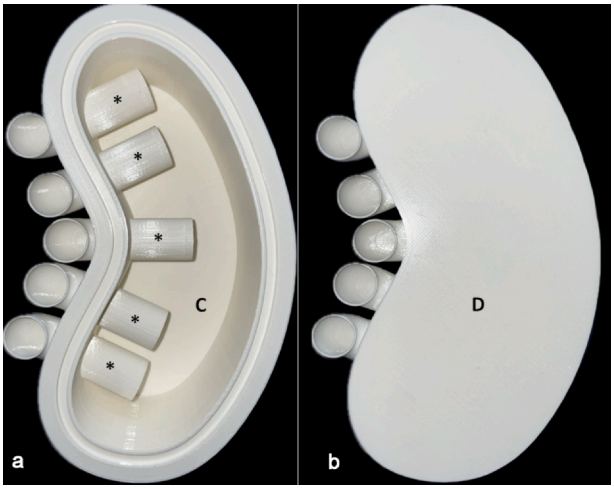

Figure 1. 3D-rendering of the custom-made 3D-printed kidney phantom. Kidney stones and contrast medium were placed into five hollow cylinders representing renal calyces (**a**, asterisk). The calyces were surrounded by a hollow chamber which was filled with distilled water (**a, C**). A 3D-printed lid was placed on top of the model to ensure an airtight seal (**b, D**).

($CTDI_{vol}$) of 5, 10, and 15 mGy for each tube voltage setup. Automated tube current modulation (CARE Dose4D, Siemens Healthcare) was used. Each scan was performed twice for a total of 24 CT scans.

Image Reconstruction

All datasets were reconstructed in the axial plane using quantum iterative reconstruction (QIR; Siemens) at a strength level of 4. We chose this setting as per vendor recommendation and because previous studies have demonstrated that a high strength level is associated with increased detection rates as well as improved image quality without compromising image texture or CT attenuation values. (12–14) The slice thickness was 2 mm and the increment was 1.6 mm. All scan setups were reconstructed as VNI and VNC images using a quantitative kernel (Qr36). VNI images were additionally reconstructed at two different energy levels of 60 keV and 70 keV as recommended by the vendor. A total of 72 CT datasets were reconstructed for analysis.

Subjective Assessment of Image Quality, Contrast Media and Iodine Subtraction

Two blinded radiologists (A.M.T.G., 3 years of experience as a radiologist and with multi-energy CT / K.M., 9 years of experience and with multi-energy CT) evaluated the overall image quality of VNI and VNC images using a five-point visual scale, whereby 5 indicates excellent image quality, 4 good image quality, 3 moderate image quality but sufficient for diagnosis, 2 poor image quality (diagnostic confidence substantially reduced) and 1 nondiagnostic.

The readers were also asked to evaluate how well contrast media was subtracted in each individual phantom cylinder/calyx using a three-point visual scale, whereby 2 indicates complete contrast subtraction, 1 incomplete contrast subtraction and 0 no contrast subtraction. In addition, the readers determined whether the kidney stone was erroneously subtracted in each individual cylinder/calyx by comparing the kidney stones in the VNI / VNC images to the kidney stones in the contrast-enhanced images using a three-point visual scale, whereby 2 indicates complete stone subtraction (no stone visible), 1 partial stone subtraction (stone only partially visible compared to the contrasted image) and 0 no stone subtraction (stone completely visible) (Fig. 2 and 3). Readers were given the option to assess the images using multiplanar reformations and a manual window setting. The readers had access to the contrast-enhanced images while reading the VNC and VNI images.

Statistical Analysis

Quantitative, normally distributed variables were reported in means and standard deviations; variables with non-normal distributions were reported in medians and interquartile ranges. Categorical variables were summarized by using frequencies and percentages. Krippendorff's α was calculated to assess inter-reader agreement. The following scale was used to assess inter-reader agreement: alpha-value between 0.0 and 0.2: slight agreement; between 0.21 and 0.4: fair agreement; between 0.41 and 0.6 moderate agreement; between 0.6 and 0.8 substantial agreement, 0.81 and 1.0: near perfect agreement. Chi-squared test was used to compare ordinal data. A p-value of < 0.05 was considered to indicate statistical significance. All statistical analyses were performed with SPSS 25 (IBM SPSS Statistics; Armonk, NY: IBM Corp).

RESULTS

Subjective Image Quality

Results of the subjective image quality rating are given in **Supplemental Digital Content** Fig. S1. Inter-reader

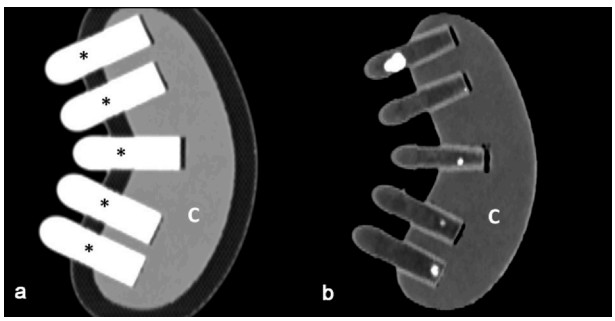

Figure 2. Coronal CT reconstruction of the kidney phantom. Prior to imaging, five cylinders representing renal calyces (**a**, asterisk) were filled with iodinated contrast and a single stone was placed into each individual calyx. A hollow chamber surrounding the cylinders/calyces was filled with distilled water **(c)**. In this example, all Calcium Oxalate stones are clearly visible within the individual calyces in the virtual non-contrast image **(b)**.

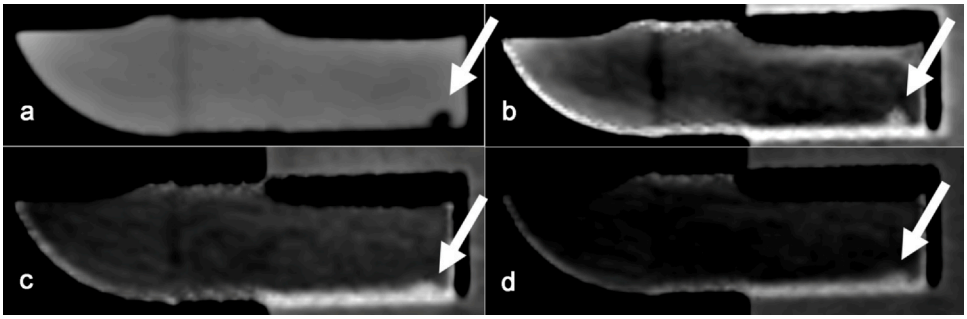

Figure 3. Example of partial kidney stone subtraction. The scan was performed with a tube voltage of 140 keV, 15 mGy dose, quantitative kernel Qr36 and quantum iterative reconstruction at a strength of 4. Axial reconstruction of the cylinder/calyx demonstrates that the 4 mm uric acid stone is clearly visible on the initial scan (**a**, arrow) and in the virtual non-contrast image (**b**, arrow). The same stone is partially subtracted in the virtual non-iodine images at 60 keV (**c**, arrow) and 70 keV (**d**, arrow).

agreement for all subjective image quality readings was fair (Krippendorff's $\alpha = 0.240$). Inter-reader agreement for image quality of VNC was near perfect (Krippendorff's $\alpha = 0.992$) but only slight for VNI (Krippendorff's $\alpha = 0.047$).

All images were rated as diagnostic. Overall image quality was rated higher for VNI compared to VNC by Reader 2 (4.9 vs. 4.0; $P < .05$). There was no significant difference in overall image quality ratings between VNI and VNC for Reader 1 (4.96 vs. 5.00; $P > .05$). Overall image quality was rated slightly lower for images acquired with a tube voltage of 120 kV as compared to 140 kV by Reader 1 (4.9 vs. 5.0; $P < .05$). Radiation dose was not significantly associated with subjective image quality for both readers ($P > .05$).

Contrast Media Subtraction

Results of the contrast media subtraction are summarized in Figure 4. Inter-reader agreement for contrast media subtraction was substantial for both VNC and VNI (Krippendorff's $\alpha = 0.628$ and 0.731). Incomplete contrast subtraction was observed significantly more frequently for VNI as compared to VNC by Reader 1 (29% vs. 15%; $P < .05$). For Reader 2, incomplete contrast subtraction was also observed more often for VNI, however this result was not statistically significant (24% vs. 20%; $P > .05$). Tube voltage and radiation dose were not associated with the degree of contrast media subtraction for both readers ($P > .05$). No virtual image was rated as having no contrast subtraction.

Kidney Stone Subtraction

Inter-reader agreement for kidney stone subtraction was substantial for both VNC and VNI (Krippendorff's $\alpha = 0.748$ and 0.668). Uric acid stones were subtracted more frequently than CaOx stones on both VNC and VNI for Reader 1 (26% complete subtraction, 13% partial subtraction and 62% no subtraction for uric acid vs. 0% complete subtraction, 1% partial subtraction and 99% no subtraction for CaOx, respectively; $P < .05$) and for Reader 2 (20% complete subtraction, 21% partial subtraction and 59% no subtraction for uric acid vs. 0% complete subtraction, 0% partial subtraction and 100% no subtraction for CaOx, respectively; $P < .05$) (Fig 5). Overall, stones were subtracted more frequently with VNI compared to VNC for both readers (Reader 1: 22% vs. 16%; Reader 2: 25% vs. 10%; $P < .05$) (Fig 6).

Smaller stones were subtracted more frequently than larger stones for both VNI and VNC images for both readers (**Supplemental Digital Content** Fig. S2; $P < .05$). Radiation dose and tube voltage were not associated with the degree of stone subtraction for both readers ($P > .05$).

DISCUSSION

This study evaluated the accuracy of contrast media subtraction and the visibility of kidney stones in excretory phase PCD-CT in a 3D printed kidney phantom, using two distinct multi-energy-based algorithms at different tube voltages and radiation doses.

With the introduction of PCD-CT into clinical practice, multi-energy-specific VNC and VNI algorithms have become clinically available. VNI uses iodine and calcium while VNC uses iodine and water as base materials for the material decomposition. To date, no study has comparatively analyzed the effectiveness of VNI and VNC in terms of contrast media subtraction and kidney stone visibility in excretory phase CT of the upper urinary tract. Our study demonstrated more frequent incomplete contrast media subtraction and partial kidney stone subtraction with VNI for both readers, regardless of the stone type. This was unexpected as VNI theoretically enhances spectral discrimination between iodine and calcium, the primary components of its decomposition algorithm. A possible explanation is that VNI's performance diminishes with high iodine concentrations or elevated CT attenuation, as indicated by our study's average CT attenuation of approximately 916 HU in the renal calyces. Further investigation into VNI's efficacy relative to iodine concentration is warranted. Additionally, differences in material decomposition algorithms between VNI and VNC, as well as potential density variations between CaOx and uric acid stones compared to traditional vessel calcifications, might have contributed to these findings.

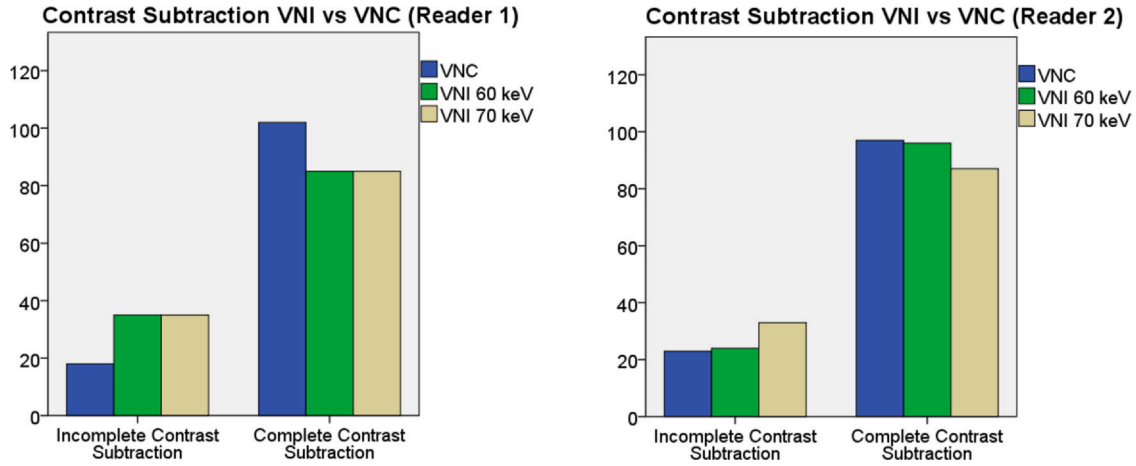

Figure 4. Degree of contrast subtraction for virtual non-iodine and virtual non-contrast. Incomplete contrast subtraction was observed significantly more frequently for VNI as compared to VNC by reader 1. For reader 2, incomplete contrast subtraction was also observed more often for VNI, however, this result was not statistically significant.

Emrich et al (15) compared true non-contrast (TNC), VNC, and VNI for coronary calcium scoring in a phantom model and in patients. The authors concluded that VNI did not detect calcifications with very low densities as compared to TNC. In addition, Turrion et. al. (16) demonstrated that small calcifications in the vessel wall of aortic aneurysms may erroneously be subtracted with VNI and may lead to false positive interpretation of endoleaks in patients who underwent endovascular aneurysm repair (EVAR). The generally lower density of CaOx and uric acid stones, compared to the higher densities (> 1000 HU) seen in vessel walls or bones, could explain the more frequent subtraction of stones with VNI in our study. Still, using VNC, incomplete contrast media subtraction occurred in up to 20%, and partial stone subtraction in up to 16% of cases.

Our findings also revealed that smaller stones (< 5 mm) were more frequently subtracted. This is a finding that has also been observed using virtual unenhanced images from the excretory phase generated with energy-integrating detector dual-energy CT. (3,17) Karlo et. al. found that detection of urinary stones < 4 mm on virtual unenhanced images was limited and the study by Takahashi et. al. demonstrated that only 29% of kidney stones with a diameter of 1–2 mm were detected on virtual unenhanced images. These findings further highlighting the influence of stone size on subtraction extent.

Dane et. al compared the degree of iodine removal in PCD-CT urographic phase-derived VNC images obtained at 120 and 140 kV (18). The authors demonstrated that VNC obtained at 140 kV showed superior iodine removal compared to 120 kV, however, they did not assess the performance of VNI. In addition, visibility of kidney stones was not directly assessed but instead a theoretical diagnostic confidence score for the identification or exclusion of urinary calculi was used. Contrarily, our study found no significant association between tube voltage, radiation dose, and the extent of iodine or stone subtraction for both VNC and VNI. This supports the trend towards low-dose protocols in

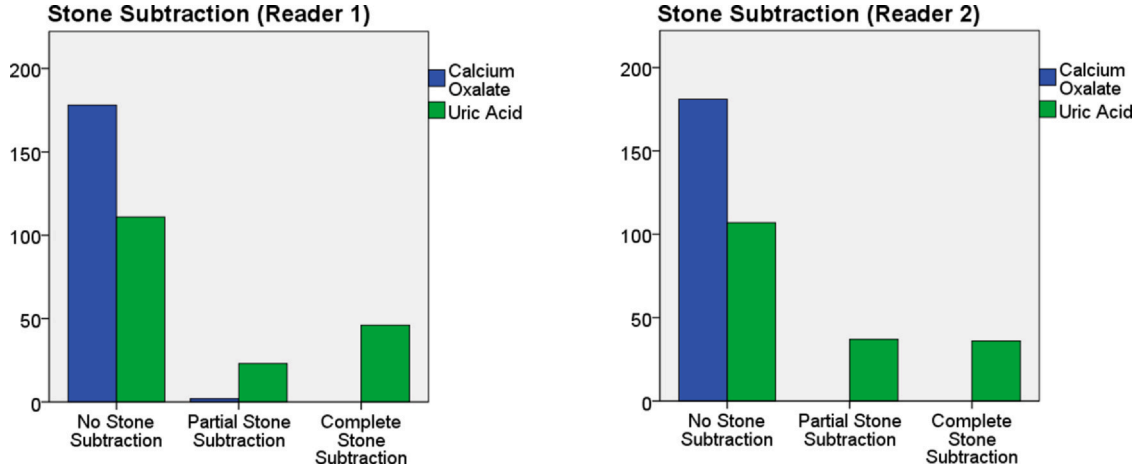

Figure 5. Degree of stone subtraction by stone type. Uric acid stones were subtracted more frequently than Calcium Oxalate stones on both virtual non-contrast and virtual non-iodine for both readers.

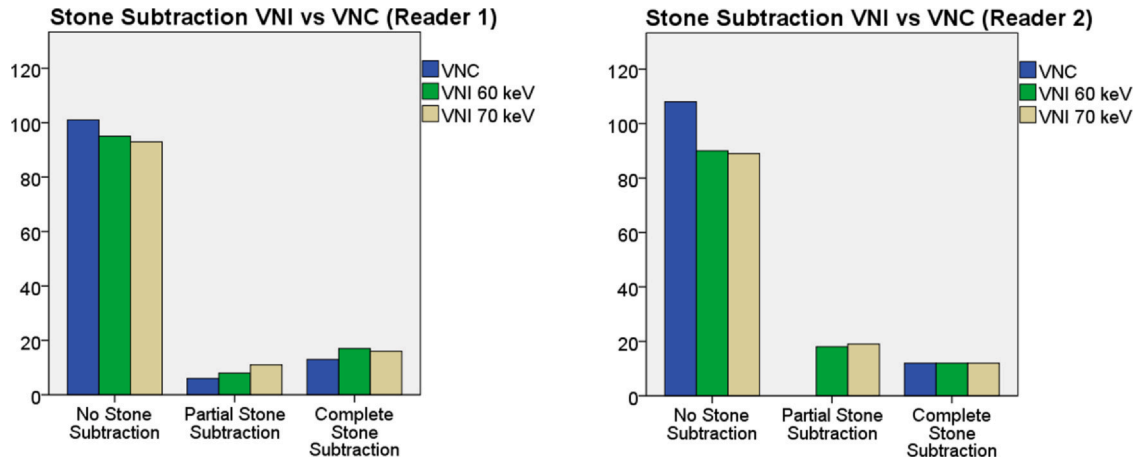

Figure 6. Degree of stone subtraction by algorithm. Overall, stones were subtracted more frequently with virtual non-iodine compared to virtual non-contrast for both readers.

kidney stone imaging, maintaining high sensitivity and specificity even with reduced radiation doses. (19,20).

Subjective image quality was rated higher for VNI as compared to VNC by one reader. This is in line with results of a study by Decker et. al (21). in which VNI was rated subjectively superior compared to VNC in patients after EVAR on PCD-CT. Interestingly, the inter-reader agreement for image quality was only slight for VNI in our study which might be a consequence of the unfamiliarity of the readers' image perception for this novel reconstruction algorithm.

Our study has several limitations. First, we used a phantom model to assess the performance of VNI and VNC which does not reflect true tissue heterogeneity or dynamic tissue properties of humans. Second, we only used two keV energies for the VNI images. Third, only a limited number of kidney stones were investigated, which may not accurately represent a wide range of stone sizes and densities. Furthermore, we only focused our analysis on two individual stone types. Forth, we did not compare VNC images from PCD-CT to VNC images from energy-integrating detector CT. Fifth, we only included a limited number of readers which may have caused the fair inter-reader agreement for all subjective image quality readings. Sixth, minor differences in the stone shape may have played a role in the degree of stone subtraction.

In conclusion, VNC demonstrated greater accuracy than VNI for contrast media subtraction and kidney stone visibility. Nonetheless, both methods still exhibited frequent incomplete contrast media subtraction and partial kidney stone subtraction, indicating the need for further research to determine if VNC from PCD-CT can effectively replace true unenhanced images in excretory phase imaging of patients.

DISCLOSURES

Diagnostic and Interventional Radiology of the University Hospital Zurich received institutional grants from Bayer Healthcare AG, Canon, Guerbet, and Siemens Healthcare GmbH unrelated to this study. In addition, André Euler and Hatem Alkadhi are part of the speaker's bureau of Siemens. Other authors declare that the research was conducted in the absence of any commercial or financial relationships that could be construed as a potential conflict of interest.

DECLARATION OF COMPETING INTEREST

The authors declare the following financial interests/personal relationships which may be considered as potential competing interests: Andre Euler reports a relationship with SIEMENS that includes: speaking and lecture fees. Hatem Alkadhi reports a relationship with SIEMENS that includes: speaking and lecture fees. If there are other authors, they declare that they have no known competing financial interests or personal relationships that could have appeared to influence the work reported in this paper.

APPENDIX A. SUPPORTING INFORMATION

Supplementary data associated with this article can be found in the online version at doi:10.1016/j.acra.2024.04.002.

REFERENCES

1. Tan WS, Feber A, Sarpong R, et al. Who should be investigated for haematuria? Results of a contemporary prospective observational study of 3556 patients. Eur Urol 2018; 74(1):10–14.
2. Expert Panel on Urological Imaging, Wolfman DJ, Marko J, et al. ACR Appropriateness Criteria® Hematuria. J Am Coll Radiol 2020; 17(5S):S138–S147.
3. Karlo CA, Gnannt R, Winklehner A, et al. Split-bolus dual-energy CT urography: protocol optimization and diagnostic performance for the detection of urinary stones. Abdom Imaging 2013; 38(5):1136–1143.
4. Mangold S, Thomas C, Fenchel M, et al. Virtual nonenhanced dual-energy CT urography with tin-filter technology: determinants of detection of urinary calculi in the renal collecting system. Radiology 2012; 264:119–125.
5. Takahashi N, Vrtiska TJ, Kawashima A, et al. Detectability of urinary stones on virtual nonenhanced images generated at pyelographic-phase dual-energy CT. Radiology 2010; 256:184–190.

6. Takahashi N, Hartman RP, Vrtiska TJ, et al. Dual-energy CT iodine-subtraction virtual unenhanced technique to detect urinary stones in an iodine-filled collecting system: a phantom study. Am J Roentgenol 2008; 190:1169–1173.
7. Scheffel H, Stolzmann P, Frauenfelder T, et al. Dual-energy contrast-enhanced computed tomography for the detection of urinary stone disease. Invest Radiol 2007; 42:823–829.
8. Marcus RP, Fletcher JG, Ferrero A, et al. Detection and characterization of renal stones by using photon-counting-based CT. Radiology 2018; 289(2):436–442.
9. Roessl E, Proksa R. K-edge imaging in x-ray computed tomography using multi-bin photon counting detectors. Phys Med Biol 2007; 52(15):4679–4696.
10. Schlomka JP, Roessl E, Dorscheid R, et al. Experimental feasibility of multi-energy photon-counting K-edge imaging in pre-clinical computed tomography. Phys Med Biol 2008; 53(15):4031–4047.
11. Leng S, Yu L, Wang J, et al. Noise reduction in spectral CT: reducing dose and breaking the trade-off between image noise and energy bin selection. Med Phys 2011; 38(9):4946–4957.
12. Sartoretti T, Landsmann A, Nakhostin D, et al. Quantum iterative reconstruction for abdominal photoncounting detector CT improves image quality. Radiology 2022; 304(3):E55.
13. Sartoretti T, Racine D, Mergen V, et al. Quantum Iterative Reconstruction for Low-Dose Ultra-High-Resolution Photon-Counting Detector CT of the Lung. Diagnostics ((Basel)) 2022; 12(2):522.
14. Racine D, Mergen V, Viry A, et al. Photon-counting detector CT for liver lesion detection-optimal virtual monoenergetic energy for different simulated patient sizes and radiation doses. Invest Radiol 2024. Epub ahead of print.
15. Emrich T, Aquino G, Schoepf UJ. Coronary computed tomography angiography-based calcium scoring: in vitro and in vivo validation of a novel virtual noniodine reconstruction algorithm on a clinical, first-generation dual-source photon counting-detector system. Invest Radiol 2022; 57:536–543.
16. Turrion AM, Mergen V, Sartoretti T, et al. Photon-counting detector CT angiography for endoleak detection after endovascular aortic repair: triphasic CT with true noncontrast versus biphasic CT with virtual noniodine imaging. Invest Radiol 2023; 58(11):816–821. 1.
17. Takahashi N, Vrtiska TJ, Kawashima A, et al. Detectability of urinary stones on virtual nonenhanced images generated at pyelographic-phase dual-energy CT. Radiology 2010; 256(1):184–190.
18. Dane B, Freedman D, Qian K, et al. Photon-counting CT urogram: optimal acquisition potential (kV) determination for virtual noncontrast creation. Abdom Radiol (NY) 2023. https://doi.org/10.1007/s00261-023-04113-7. Epub ahead of print.
19. Drake T, Jain N, Bryant T, et al. Should low-dose computed tomography kidneys, ureter and bladder be the new investigation of choice in suspected renal colic? A systematic review. Indian J Urol 2014; 30(2):137–143.
20. Kunz AS, Grunz JP, Halt D, et al. Tin-filtered 100 kV Ultra-low-dose Abdominal CT for Calculi detection in the urinary tract: a comparative study of 510 cases. Acad Radiol 2023; 30(6):1033–1038.
21. Decker JA, Bette S, Scheurig-Muenkler C, et al. Virtual non-contrast reconstructions of photon-counting detector CT angiography datasets as substitutes for true non-contrast acquisitions in patients after EVAR-performance of a novel calcium-preserving reconstruction algorithm. Diagn Basel Switz 2022; 12:558.